ChemComm

Accepted Manuscript

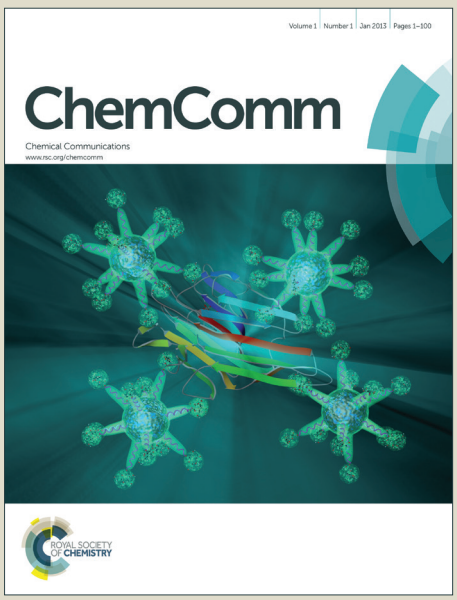

ROYAL SOCIETY OF CHEMISTRY

www.rsc.org/chemcomm

Cite this: DOI: 10.1039/c0xx00000x

www.rsc.org/xxxxxx

ARTICLE TYPE

Supramolecular Co(II)$_{14}$-Metal-Organic Cube in a Hydrogen-Bonded Network and a Co(II)-Organic Framework with Flexible Methoxy Substituent

Suvendu Sekhar Mondal,[a] Asamanjoy Bhunia,[b] Alexandra Kelling,[a] Uwe Schilde,[a] Christoph Janiak,[b] and Hans-Jürgen Holdt*[a]

Received (in XXX, XXX) Xth XXXXXXXXX 20XX, Accepted Xth XXXXXXXXX 20XX
DOI: 10.1039/b000000x

The reaction of 4,5-dicyano-2-methoxyimidazole (L1) with Co(NO$_3$)$_2$·6H$_2$O under solvothermal conditions in DMF, a MOF, IFP-8 and hydrogen-bonded network consisting of tetradecanuclear Co(II)$_{14}$-metal organic cube (1) are formed. 1 shows the bcu net with 14 cobalt atoms.

To design of new solid-state materials, supramolecular chemistry is of great interest because it takes advantage of self-assembly to synthesized new materials by virtue of cooperative interactions such as ion-ion interactions, hydrogen bonding, dipole-dipole interactions and aromatic π-π interaction.[1-6] Moreover, the flexible or soft porous networks, also known the third generation of porous coordination polymers, receive much attention because of their interesting properties.[7,8] Flexible metal-organic frameworks (MOFs) are extremely interesting for applications in selective gas adsorption/separation or chemical sensing.[8] Such frameworks exhibit guest dependent structural transformation and breathing effect.[9]

However, our group succeeded in a particular approach in obtaining the zinc based isoreticular IFP series (IFP = imidazolate framework Potsdam) by replacing the substituent of R-group of 2-substituted imidazolate 4-amide-5-imidate linker (–R = CH_3, C_2H_5, Cl, Br).[10-12] To extend the number of frameworks at isoreticular series of IFP, recently, we reported a Zn-based material, known as IFP-7 that showed the gate-effects due to flexible methoxy substituent of the linker.[11] In addition to IFP-7, an *in situ* imidazolate-4,5-diamide-2-olate (L3) linker based Zn$_{14}$-molecular building block (MBB) is also formed.[13] These MBBs or specifically metal-organic cubes (MOCs) contain the peripheral H-bonding substituents that construct an effective way to H-bonded supramolecular networks with channels and pores.[5,6,13] Hence, to achieve such kind of a rigid and directional single-metal-ion based MBB based supramolecular assemblies, the solvothermal reactions with such linker precursor and other metal salts can be explored. Herein, we report a cube-like Co$_{14}$-MOC are engaged into amide-amide H-bonds (denoted as **1**), forming a supramolecular network (Fig. 1b) which is similar with Zn$_{14}$-MBB and a imidazolate-4-amide-5-imidate based MOF (named as **IFP-8**, Fig. 1d) shows the flexibility due to methoxy substituent.

H-bonded MOCs based supramolecular network (**1**) is formed from *in situ* hydrolysis of the ligand precursor 4,5-dicyano-2-methoxyimidazole (L1). Under solvothermal condions in *N, N'*-dimethylformamide (DMF), partial hydrolysis of the cyano groups to amide groups and of the methoxy to the hydroxy group followed by twofold deprotonation generate L3 linker (Schemes 1 and S1, at ESI†). The linker L3 is only stable in the deprotonated and metal-coordinated state because the free ligand H$_2$L3 irreversibly transforms to a stable tautomeric keto-form. Under this reaction condition, in addition to **1**, another *in situ* functionalizaing 2-methoxyimidazolate-4-amide-5-imidate (L2) linker based material, **IFP-8** is formed as a main product (Scheme 1 and ESI†). **IFP-8** was separated by sieving technique,[14] wherein **1** was trapped by a mesh while **IFP-8** filtered through it. After several attempts, we could not find a suitable crystal of **IFP-8** for single X-ray diffraction. Hence, the structure was determined by a combination of Powder X-ray diffraction (PXRD), structure modelling and IR spectroscopy (Fig. 1d). The structural model of **IFP-8** was constructed by using the single-crystal X-ray structure determination for IFP-1,[10a] and was further optimized by using a density functional theory *ab initio* method (see ESI†). The PXRD pattern of the optimised **IFP-8** structure shows very good agreement with the experimental data (Fig. S10, ESI†).

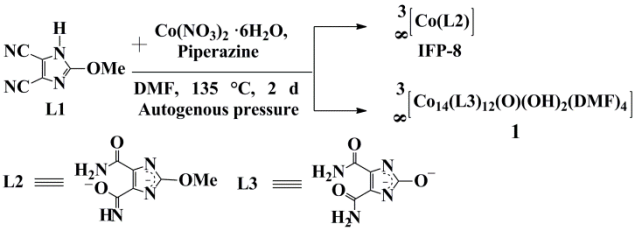

Scheme 1 Syntheses of **1** and **IFP-8**. *In situ* imidazolate-4,5-diamide-2-olate (L3) linker, synthesis with indication of its cobalt coordination (Fig. S3) and H-bonds in **1**. See ESI† for experimental details.

Compound **1** was characterized by single-crystal X-ray diffraction as $[Co_{14}(L3)_{12}(O)(OH)_2(DMF)_4]\cdot(DMF)_{16}$ for the asymmetric unit.[15] The degree of *in situ* hydrolysis of the cyano groups of L1 into the corresponding L3 linker was studied with infrared (IR) spectroscopy (see ESI†). Compound **1** crystallizes

in the high-symmetry space group *I*4/*m* of the tetragonal crystal system. Twelve L3 ligands, one oxide ion, two hydroxide ions and four DMF molecules assemble with fourteen cobalt ions to a tetradecanuclear Co_{14}-MOC with peripherial amide groups (Fig. 1a). Whereas H-bonded Zn_{14}-MBB network. possesses the space group *Ia*-3*d* (No 230), having highest crystallographic symmetry and contains four water molecules, instead of four DMF.[13] The oxide ion (O1) is located in the centre of the MOC, surrounded by four Co1 and two Co2 atoms in an exact octahedral coordination environment (Fig. 1a and 4Sb). Each of these four Co1 atoms is further coordinated by four olate oxygen atoms of four imidazolate ligands (two O2 and two O3), one O^{2-} (O1) and one DMF (O4) forming a distorted octahedral coordination geometry (Fig. S5, ESI†). The two Co2 centres are surrounded by four olate oxygen atoms (O2), one O^{2-} (O1) and one DMF (O5) to form a distorted octahedral coordination geometry (Fig. S5, ESI†). Eight Co3 atoms are each coordinated by three nitrogen atoms (N1, N2 and N5) from two imidazolate ligands, two amide oxygen atoms (O6 and O8) and an olate ion (O2) as linker in a twofold face-capped tetrahedron (Fig. S5, see ESI†). The metal ion at **IFP-8** structure is penta-coordinated by the L2 linkers to form a distorted trigonal-bipyramidal geometry (Fig. S7, ESI†). The structure possesses 1D hexagonal channels running along 0, 0, z; 1/3, 2/3, z and 2/3, 1/3, z. The methoxy groups protrude into the open channels and determine their accessible diameter (Fig. 1d). By considering the van der Waals radii, a probable channel diameter of the channels in was estimated to be 1.9 Å (see ESI† for details).

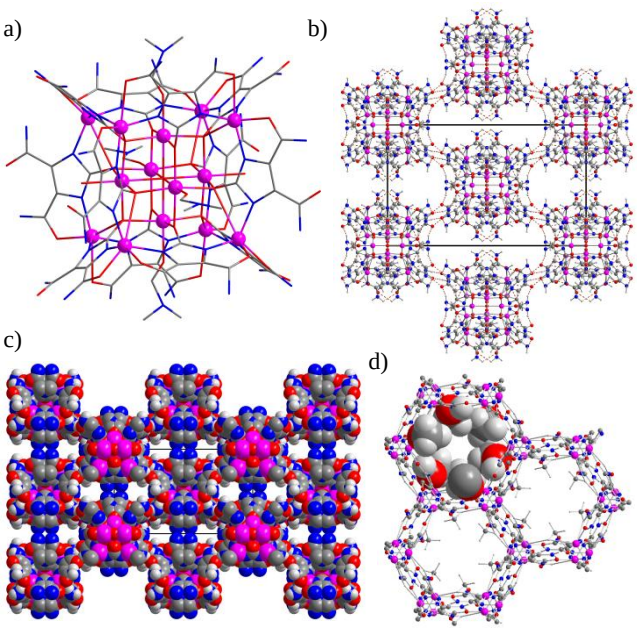

Fig. 1 (a) Tetradecanuclear cobalt MOC of **1**; (b) hydrogen-bonded supramolecular assembly of **1**, view along *a* axis; (c) space filling model of **1**; (d) hexagonal channels in **IFP-8**, the methoxy substituent at the linker L2 is presented in a space filling mode. The structure is based on density functional *ab initio* calculations (pink Co, blue N, red O, dark gray C, light gray H).

The MOC of **1** contains at its vertices and edges coordinated and free amide groups. These are involved in intramolecular hydrogen bonds of L3 and intermolecular hydrogen bonds between the MOCs or protrude into the channels of **1**. The intramolecular hydrogen bonds (N3–H3B···O7 = 2.68 Å) stabilizing additionally the MOC. Each MOC is connected through its vertices with eight MOCs by intermolecular N–H···O hydrogen bonds (N(4)–H(4)A···O(7) = 2.90 Å) between the peripheral amide groups, generating the 3D-supramolecular assembly of **1** (Fig. 1b). Hence, L3 acts as bridging linkers because of their unique potential to offer the amide groups, *N*-donor sites of imidazole and olate ion when chelated to a metal ion and additionally, some amides of the MOC were employed in hydrogen-bonding with other MOCs, which are necessary for supramolecular assemblies. However, the framework exhibits two types of infinite channels. The first type of channel running along the crystallographic *c* axis has small openings with an approximate diameter of 1.7 Å (Fig. S6, ESI†), while the second type of accessible channel running along the *a* axis can accommodate a sphere with a maximum diameter of 3.2 Å given the van-der-Waals radii of the nearest atoms (Fig. 1c). Hence, guest molecules such as DMF can be hydrogen-bonded by potential donors and acceptors amide functionality.

The topology of **1** can be described as hydrogen-bonded 8-c body-centered cubic (**bcu**) net with the nodes Co_{14}-MOCs (Fig. S9, ESI†). Moreover, the Co_{14}-MOC could be inscribed in a cube, one can also describe the net as the augmented version of **bcu** (= **bcu-a**) that is called polycubane (**pcb**).[13] In contrast, Co^{2+} ions at **IFP-8** and bridging ligands L2 act as 3-connected topological species forming a net with a rare uninodal topology, named *etb*. The topology of IFP-8 is classified by the vertex symbol 3.6.10.15.[10]

PXRD pattern of activated **IFP-8** exhibited the sharp diffraction peaks similar to that as-synthesized sample. This indicates that the porous framework is maintained the crystalline integrity even without solvent molecules (Fig. S10, ESI†).

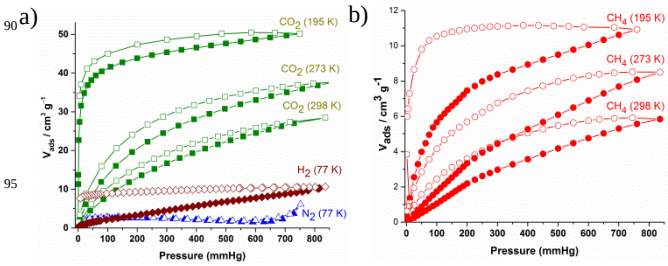

Fig. 2 Gas sorption isotherms for activated **IFP-8**. Adsorption and desorption branches are indicated by closed and open symbols, respectively.

The activated **IFP-8** is expected to show the gas-sorption selectivity towards small polar molecules due to its polar and flexible methoxy side chains. The gas sorption isotherms are recorded for N_2, H_2, CH_4, and CO_2 gases at various temperatures at 1 bar (Fig. 2). Moreover, we are unable to examine the gas uptake capacities as well as other physical properties for compound **1** in the present study due to low yield. We are engaged to optimize the synthetic condition for better yield. As indicated in Fig. 2a, **IFP-8** barely adsorbed N_2, which can be attributed to a gating of the pores by the pendant 2-methoxy groups, while the CO_2, CH_4 and H_2 sorption isotherms show very different sorption behaviors.[9,11] The CO_2 sorption measurements

at 195, 273 and 298 K show typical type I isotherms and a small hysteresis is visible in all the desorption branches, indicating that the framework structure containing the flexible substituent. Such hysteretic behavior of **IFP-8** is similar with zinc based imidazolate-4-amide-5-imidate (L2) frameworks IFP-7 and other MOFs, having flexible alkoxy substituents.[9,11] The uptake of CO_2 by **IFP-8** at 298 K and 1 bar is 27 $cm^3\ g^{-1}$ and the uptake of CO_2 by IFP-7 is 40 $cm^3\ g^{-1}$. However, 2-methylimidazolate-4-amide-5-imidate linker based isostructural frameworks Zn-based IFP-1[10a] and Co-based IFP-5 were reported.[12] The channel diameter of IFP-5 (3.8 Å) is slightly lower than that of IFP-1 (4.2 Å); hence, the gas uptake capacities and BET surface area are slightly lower than IFP-1. Similarly, the channel diameter of Co-based **IFP-8** is slightly narrower than the Zn-based IFP-7. Hence, it can be inferred that the gas uptake capacities for **IFP-8** are much less than IFP-7. IFPs structures contain 1D hexagonal channel and the gas uptake capacities depend on the size of the channel. In contrast CO_2 uptake capacities of Co-based ZIFs (Co-ZIF-68, -69, -81) are higher than their isostructural with Zn based analogues (Zn-ZIF-68, -69 and -81).[16] In such frameworks, the interaction with CO_2 presumably increases inside the Co based ZIFs compared to their Zn based analogues due to decreased ionic radius [Zn^{+2} (0.68 Å) and Co^{+2} (0.67 Å)] and the low density of Co-ZIFs.[16] The isosteric heats of adsorption were calculated from the CO_2 adsorption isotherms at 273 K and 298 K (Fig. 2a). At zero loading the Q_{st} value ($-\Delta H$) for **IFP-8** is 37 kJ mol^{-1} (Fig. S12, ESI†), comparable to other MOFs.[8b] Upon increasing the loading the Q_{st} value is decreases to 24 kJ mol^{-1}. The high Q_{st} value can be attributed to the highly polar framework and the effect of the small pore size effect.

Remarkably, the desorption branches for CH_4 isotherms show a wide desorption hysteresis which is very similar with IFP-7. **IFP-8** adsorbs 11 $cm^3\ g^{-1}$ CH_4 at 195 K and 1 bar (Fig. 2b). The CH_4 desorption isotherm at 195 K confirms that 85 % of the adsorbed CH_4 is trapped in the framework when the pressure is reduced form 760 mmHg to 75 mmHg, and 71 % of the adsorbed CH_4 remains when the pressure further reduced to 25 mmHg. Such a broad desorption behaviour for CH_4 isotherm at atmospheric pressure is rarely observed in microporous MOFs.[11,17] After CH_4 uptake the PXRD pattern of **IFP-8** maintained its structural integrity. The structural transformation was not occurred (Fig. S10, ESI†). Another agreeable example that has proven the flexibility of the framework is by H_2 sorption. **IFP-8** adsorbs 9.3 $cm^3\ g^{-1}$ of H_2 at 77 K and 1 bar (Fig. 2a), showing a wide desorption hysteresis. Moreover, we determined the initial slopes in the Henry region of the adsorption isotherms of **IFP-8** (Fig. S13, ESI†). The adsorption selectivities of **IFP-8** are 34:1 and 9:1 for CO_2/N_2 and CO_2/CH_4, respectively, wherein the adsorption selectivities of IFP-7 are 37:1 and 7:1 for CO_2/N_2 and CO_2/CH_4, respectively at 273 K and 1 bar.[11]

In conclusion, not only zinc can formed H-bonded supramolecular assembly but also cobalt yielded a large Co_{14}-MOC via *in situ* functionalization of unusual linker generation under solvothermal condition. The cobalt atoms in the Co_{14}-MOC formed Co_6 octahedron inscribed distorted Co_8 cube ($Co_6@Co_8$). However, **1** shows the **bcu** net with 14 cobalt atoms. Due to flexible methoxy substituent, the hysteretic sorption behavior for **IFP-8** indicates a flexible MOF. **IFP-8** exhibits the gas sorption selectivity.

We thank Dr. I. A. Baburin (Institut für Physikalische Chemie und Elektrochemie, Technische Universität Dresden, Dresden, Germany) for theoretical calculations for **IFP-8**. This work is financially supported by the Priority Program 1362 of the German Research Foundation on "Metal-Organic Frameworks."

Notes and references

1 J. W. Steed and J. L. Atwood in *Supramolecular Chemistry*, 2nd Edition, Wiley-VCH, Weinheim, Germany, 2009.

2 (*a*) L. R. MacGillivray in *Metal-Organic Frameworks: Design and Application*, John Wiley & Sons, Hoboken, NJ, 2010; (*b*) D. Farrusseng, in *Metal-Organic Frameworks Applications from Catalysis to Gas Storage*, Wiley-VCH, Weinheim, Germany, 2011.

3 C.-L. Chen and A. M. Beatty, *J. Am. Chem. Soc.*, 2008, **130**, 17222–17223.

4 G. A. Hogan, N. P. Rath and A. M. Beatty, *Cryst. Growth Des.*, 2011, **11**, 3740–3743.

5 D. F. Sava, V. Ch. Kravtsov, J. Eckert, J. F. Eubank, F. Nouar and M. Eddaoudi, *J. Am. Chem. Soc.*, 2009, **131**, 10394–10396.

6 S. Wang, T. Zhao, G. Li, L. Wojtas, Q. Huo, M. Eddaoudi and Y. Liu, *J. Am. Chem. Soc.*, 2010, **132**, 18038–18041.

7 (*a*) S. Kitagawa and K. Uemura, *Chem. Soc. Rev.*, 2005, **34**, 109−119; (*b*) G. Férey and C. Serre, *Chem. Soc. Rev.*, 2009, **38**, 1380−1399.

8 (*a*) J.-R. Li, J. Sculley and H.-C. Zhou, *Chem. Rev.*, 2012, **112**, 869−932; (*b*) L. E. Kreno, K. Leong, O. K. Farha, M. Allendorf, R. P. Van Duyne and J. T. Hupp, *Chem. Rev.*, 2012, **112**, 1105−1125.

9 (*a*) S. Henke, A. Schneemann, A. Wütscher and R. A. Fischer, *J. Am. Chem. Soc.*, 2012, **134**, 9464−9474; (*b*) S. Henke and R. A. Fischer, *J. Am. Chem. Soc.*, 2011, **133**, 2064–2067.

10 (*a*) F. Debatin, A. Thomas, A. Kelling, N. Hedin, Z. Bacsik, I. Senkovska, S. Kaskel, M. Junginger, H. Müller, U. Schilde, C. Jäger, A. Friedrich and H.-J. Holdt, *Angew. Chem. Int. Ed.*, 2010, **49**, 1258–1262; (*b*) F. Debatin, K. Behrens, J. Weber, I. A. Baburin, A. Thomas, J. Schmidt, I. Senkovska, S. Kaskel, A. Kelling, N. Hedin, Z. Bacsik, S. Leoni, G. Seifert, C. Jäger, C. Günter, U. Schilde, A. Friedrich and H.-J. Holdt, *Chem. Eur. J.*, 2012, **18**, 11630–11640.

11 S. S. Mondal, A. Bhunia, I. A. Baburin, C. Jäger, A. Kelling, U. Schilde, G. Seifert, C. Janiak and H.-J. Holdt, *Chem. Commun.*, 2013, **49**, 7599–7601.

12 S. S. Mondal, A. Bhunia, S. Demeshko, A. Kelling, U. Schilde, C. Janiak and H.-J. Holdt, *CrystEngComm.*, 2104, **16**, 39–42.

13 S. S. Mondal, A. Bhunia, A. Kelling, U. Schilde, C. Janiak and H.-J. Holdt, *J. Am. Chem. Soc.*, 2014, **136**, 44–47.

14 T. D. Keene, D. J. Price and C. J. Kepert, *Dalton Trans.*, 2011, **40**, 7122–7126.

15 Crystal data for **1**: $C_{14.50}H_{22.25}Co_{1.75}N_{8.50}O_{7.37}$, M_r = 536.78 $g{\cdot}mol^{-1}$, crystal dimensions 0.44 × 0.42 × 0.40 mm, tetragonal, space group $I4/m$(No 87), $a = b$ = 17.8029(3) Å, c = 29.2271(7) Å, V = 9263.3(4) $Å^3$, Z = 16, ρ_{calcd} = 1.54 $g{\cdot}cm^{-3}$; $\mu(Mo_{K\alpha})$ = 1.313 mm^{-1} (λ = 0.71073 Å), T = 210 K; $2\Theta_{max}$ = 25.00°, 29163 reflections measured, 4156 unique (R_{int} = 0.1056), R_1 = 0.0623, wR = 0.1750 ($I > 2\sigma(I)$).

16 T. Panda, K. M. Gupta, J. Jiang and R. Banerjee, *CrystEngComm.*, 2014, DOI: 10.1039/C3CE42075B.

17 D. Zhao, D. Yuan, R. Krishna, J. M. van Baten and H.-C. Zhou, *Chem. Commun.*, 2010, **46**, 7352–7354.

[a] *Institut für Chemie, Anorganische Chemie, Universität Potsdam, Karl-Liebknecht-Straße 24-25, 14476 Potsdam, Germany*
Fax: +49 331-977-5055; Tel: +39 331-977-5180; E-mail: holdt@uni-potsdam.de
[b] *Institut für Anorganische Chemie und Strukturchemie, Heinrich-Heine-Universität Düsseldorf, 40204 Düsseldorf, Germany*

† Electronic Supplementary Information (ESI) available: Detailed experimental procedure, IR spectra, PXRD patterns, TGA traces, table of X-ray data of **1**, gas adsorption data. CCDC 974537. See DOI: 10.1039/b000000x/‡

Cite this: DOI: 10.1039/c0xx00000x

www.rsc.org/xxxxxx

ARTICLE TYPE

Supramolecular Co(II)$_{14}$-Metal-Organic Cube in a Hydrogen-Bonded Network and a Co(II)-Organic Framework with Flexible Methoxy Substituent

Suvendu Sekhar Mondal,[a] Asamanjoy Bhunia,[b] Alexandra Kelling,[a] Uwe Schilde,[a] Christoph Janiak,[b] and Hans-Jürgen Holdt*[a]

Received (in XXX, XXX) Xth XXXXXXXXX 20XX, Accepted Xth XXXXXXXXX 20XX
DOI: 10.1039/b000000x

The reaction of 4,5-dicyano-2-methoxyimidazole (L1) with $Co(NO_3)_2{\cdot}6H_2O$ under solvothermal conditions in DMF, a MOF, IFP-8 and hydrogen-bonded network consisting of tetradecanuclear Co(II)$_{14}$-metal organic cube (1) are formed. 1 shows the bcu net with 14 cobalt atoms.

To design of new solid-state materials, supramolecular chemistry is of great interest because it takes advantage of self-assembly to synthesized new materials by virtue of cooperative interactions such as ion-ion interactions, hydrogen bonding, dipole-dipole interactions and aromatic π-π interaction.[1-6] Moreover, the flexible or soft porous networks, also known the third generation of porous coordination polymers, receive much attention because of their interesting properties.[7,8] Flexible metal-organic frameworks (MOFs) are extremely interesting for applications in selective gas adsorption/separation or chemical sensing.[8] Such frameworks exhibit guest dependent structural transformation and breathing effect.[9]

However, our group succeeded in a particular approach in obtaining the zinc based isoreticular IFP series (IFP = imidazolate framework Potsdam) by replacing the substituent of R-group of 2-substituted imidazolate 4-amide-5-imidate linker (–R = CH_3, C_2H_5, Cl, Br).[10-12] To extend the number of frameworks at isoreticular series of IFP, recently, we reported a Zn-based material, known as IFP-7 that showed the gate-effects due to flexible methoxy substituent of the linker.[11] In addition to IFP-7, an *in situ* imidazolate-4,5-diamide-2-olate (L3) linker based Zn$_{14}$-molecular building block (MBB) is also formed.[13] These MBBs or specifically metal-organic cubes (MOCs) contain the peripheral H-bonding substituents that construct an effective way to H-bonded supramolecular networks with channels and pores.[5,6,13] Hence, to achieve such kind of a rigid and directional single-metal-ion based MBB based supramolecular assemblies, the solvothermal reactions with such linker precursor and other metal salts can be explored. Herein, we report a cube-like Co$_{14}$-MOC are engaged into amide-amide H-bonds (denoted as **1**), forming a supramolecular network (Fig. 1b) which is similar with Zn$_{14}$-MBB and a imidazolate-4-amide-5-imidate based MOF (named as **IFP-8**, Fig. 1d) shows the flexibility due to methoxy substituent.

H-bonded MOCs based supramolecular network (**1**) is formed from *in situ* hydrolysis of the ligand precursor 4,5-dicyano-2-methoxyimidazole (L1). Under solvothermal condions in *N, N′*-dimethylformamide (DMF), partial hydrolysis of the cyano groups to amide groups and of the methoxy to the hydroxy group followed by twofold deprotonation generate L3 linker (Schemes 1 and S1, at ESI†). The linker L3 is only stable in the deprotonated and metal-coordinated state because the free ligand H_2L3 irreversibly transforms to a stable tautomeric keto-form. Under this reaction condition, in addition to **1**, another *in situ* functionalizaing 2-methoxyimidazolate-4-amide-5-imidate (L2) linker based material, **IFP-8** is formed as a main product (Scheme 1 and ESI†). **IFP-8** was separated by sieving technique,[14] wherein **1** was trapped by a mesh while **IFP-8** filtered through it. After several attempts, we could not find a suitable crystal of **IFP-8** for single X-ray diffraction. Hence, the structure was determined by a combination of Powder X-ray diffraction (PXRD), structure modelling and IR spectroscopy (Fig. 1d). The structural model of **IFP-8** was constructed by using the single-crystal X-ray structure determination for IFP-1,[10a] and was further optimized by using a density functional theory *ab initio* method (see ESI†). The PXRD pattern of the optimised **IFP-8** structure shows very good agreement with the experimental data (Fig. S10, ESI†).

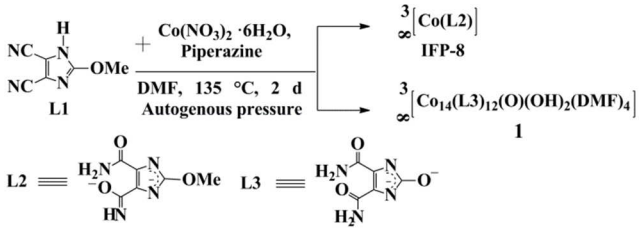

Scheme 1 Syntheses of **1** and **IFP-8**. *In situ* imidazolate-4,5-diamide-2-olate (L3) linker, synthesis with indication of its cobalt coordination (Fig. S3) and H-bonds in **1**. See ESI† for experimental details.

Compound **1** was characterized by single-crystal X-ray diffraction as $[Co_{14}(L3)_{12}(O)(OH)_2(DMF)_4]{\cdot}(DMF)_{16}$ for the asymmetric unit.[15] The degree of *in situ* hydrolysis of the cyano groups of L1 into the corresponding L3 linker was studied with infrared (IR) spectroscopy (see ESI†). Compound **1** crystallizes

in the high-symmetry space group *I4/m* of the tetragonal crystal system. Twelve L3 ligands, one oxide ion, two hydroxide ions and four DMF molecules assemble with fourteen cobalt ions to a tetradecanuclear Co_{14}-MOC with peripherial amide groups (Fig. 1a). Whereas H-bonded Zn_{14}-MBB network. possesses the space group *Ia*-3*d* (No 230), having highest crystallographic symmetry and contains four water molecules, instead of four DMF.[13] The oxide ion (O1) is located in the centre of the MOC, surrounded by four Co1 and two Co2 atoms in an exact octahedral coordination environment (Fig. 1a and 4Sb). Each of these four Co1 atoms is further coordinated by four olate oxygen atoms of four imidazolate ligands (two O2 and two O3), one O^{2-} (O1) and one DMF (O4) forming a distorted octahedral coordination geometry (Fig. S5, ESI†). The two Co2 centres are surrounded by four olate oxygen atoms (O2), one O^{2-} (O1) and one DMF (O5) to form a distorted octahedral coordination geometry (Fig. S5, ESI†). Eight Co3 atoms are each coordinated by three nitrogen atoms (N1, N2 and N5) from two imidazolate ligands, two amide oxygen atoms (O6 and O8) and an olate ion (O2) as linker in a twofold face-capped tetrahedron (Fig. S5, see ESI†). The metal ion at **IFP-8** structure is penta-coordinated by the L2 linkers to form a distorted trigonal-bipyramidal geometry (Fig. S7, ESI†). The structure possesses 1D hexagonal channels running along 0, 0, z; 1/3, 2/3, z and 2/3, 1/3, z. The methoxy groups protrude into the open channels and determine their accessible diameter (Fig. 1d). By considering the van der Waals radii, a probable channel diameter of the channels in was estimated to be 1.9 Å (see ESI† for details).

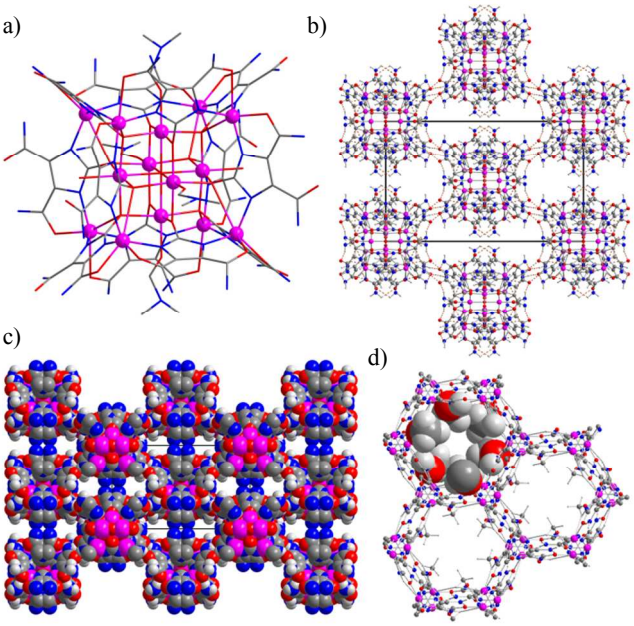

Fig. 1 (a) Tetradecanuclear cobalt MOC of **1**; (b) hydrogen-bonded supramolecular assembly of **1**, view along *a* axis; (c) space filling model of **1**; (d) hexagonal channels in **IFP-8**, the methoxy substituent at the linker L2 is presented in a space filling mode. The structure is based on density functional *ab initio* calculations (pink Co, blue N, red O, dark gray C, light gray H).

The MOC of **1** contains at its vertices and edges coordinated and free amide groups. These are involved in intramolecular hydrogen bonds of L3 and intermolecular hydrogen bonds between the MOCs or protrude into the channels of **1**. The intramolecular hydrogen bonds (N3–H3B···O7 = 2.68 Å) stabilizing additionally the MOC. Each MOC is connected through its vertices with eight MOCs by intermolecular N–H···O hydrogen bonds (N(4)–H(4)A···O(7) = 2.90 Å) between the peripheral amide groups, generating the 3D-supramolecular assembly of **1** (Fig. 1b). Hence, L3 acts as bridging linkers because of their unique potential to offer the amide groups, *N*-donor sites of imidazole and olate ion when chelated to a metal ion and additionally, some amides of the MOC were employed in hydrogen-bonding with other MOCs, which are necessary for supramolecular assemblies. However, the framework exhibits two types of infinite channels. The first type of channel running along the crystallographic *c* axis has small openings with an approximate diameter of 1.7 Å (Fig. S6, ESI†), while the second type of accessible channel running along the *a* axis can accommodate a sphere with a maximum diameter of 3.2 Å given the van-der-Waals radii of the nearest atoms (Fig. 1c). Hence, guest molecules such as DMF can be hydrogen-bonded by potential donors and acceptors amide functionality.

The topology of **1** can be described as hydrogen-bonded 8-c body-centered cubic (**bcu**) net with the nodes Co_{14}-MOCs (Fig. S9, ESI†). Moreover, the Co_{14}-MOC could be inscribed in a cube, one can also describe the net as the augmented version of **bcu** (= **bcu-a**) that is called polycubane (**pcb**).[13] In contrast, Co^{2+} ions at **IFP-8** and bridging ligands L2 act as 3-connected topological species forming a net with a rare uninodal topology, named *etb*. The topology of IFP-8 is classified by the vertex symbol 3.6.10.15.[10]

PXRD pattern of activated **IFP-8** exhibited the sharp diffraction peaks similar to that as-synthesized sample. This indicates that the porous framework is maintained the crystalline integrity even without solvent molecules (Fig. S10, ESI†).

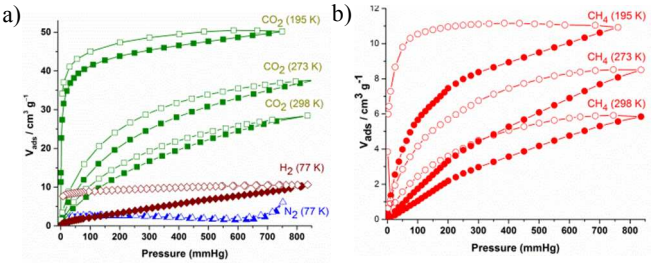

Fig. 2 Gas sorption isotherms for activated **IFP-8**. Adsorption and desorption branches are indicated by closed and open symbols, respectively.

The activated **IFP-8** is expected to show the gas-sorption selectivity towards small polar molecules due to its polar and flexible methoxy side chains. The gas sorption isotherms are recorded for N_2, H_2, CH_4, and CO_2 gases at various temperatures at 1 bar (Fig. 2). Moreover, we are unable to examine the gas uptake capacities as well as other physical properties for compound **1** in the present study due to low yield. We are engaged to optimize the synthetic condition for better yield. As indicated in Fig. 2a, **IFP-8** barely adsorbed N_2, which can be attributed to a gating of the pores by the pendant 2-methoxy groups, while the CO_2, CH_4 and H_2 sorption isotherms show very different sorption behaviors.[9,11] The CO_2 sorption measurements

at 195, 273 and 298 K show typical type I isotherms and a small hysteresis is visible in all the desorption branches, indicating that the framework structure containing the flexible substituent. Such hysteretic behavior of **IFP-8** is similar with zinc based imidazolate-4-amide-5-imidate (L2) frameworks IFP-7 and other MOFs, having flexible alkoxy substituents.[9,11] The uptake of CO_2 by **IFP-8** at 298 K and 1 bar is 27 cm^3 g^{-1} and the uptake of CO_2 by IFP-7 is 40 cm^3 g^{-1}. However, 2-methylimidazolate-4-amide-5-imidate linker based isostructural frameworks Zn-based IFP-1[10a] and Co-based IFP-5 were reported.[12] The channel diameter of IFP-5 (3.8 Å) is slightly lower than that of IFP-1 (4.2 Å); hence, the gas uptake capacities and BET surface area are slightly lower than IFP-1. Similarly, the channel diameter of Co-based **IFP-8** is slightly narrower than the Zn-based IFP-7. Hence, it can be inferred that the gas uptake capacities for **IFP-8** are much less than IFP-7. IFPs structures contain 1D hexagonal channel and the gas uptake capacities depend on the size of the channel. In contrast CO_2 uptake capacities of Co-based ZIFs (Co-ZIF-68, -69, -81) are higher than their isostructural with Zn based analogues (Zn-ZIF-68, -69 and -81).[16] In such frameworks, the interaction with CO_2 presumably increases inside the Co based ZIFs compared to their Zn based analogues due to decreased ionic radius [Zn^{+2} (0.68 Å) and Co^{+2} (0.67 Å)] and the low density of Co-ZIFs.[16] The isosteric heats of adsorption were calculated from the CO_2 adsorption isotherms at 273 K and 298 K (Fig. 2a). At zero loading the Q_{st} value (–ΔH) for **IFP-8** is 37 kJ mol^{-1} (Fig. S12, ESI†), comparable to other MOFs.[8b] Upon increasing the loading the Q_{st} value is decreases to 24 kJ mol^{-1}. The high Q_{st} value can be attributed to the highly polar framework and the effect of the small pore size effect.

Remarkably, the desorption branches for CH_4 isotherms show a wide desorption hysteresis which is very similar with IFP-7. **IFP-8** adsorbs 11 cm^3 g^{-1} CH_4 at 195 K and 1 bar (Fig. 2b). The CH_4 desorption isotherm at 195 K confirms that 85 % of the adsorbed CH_4 is trapped in the framework when the pressure is reduced form 760 mmHg to 75 mmHg, and 71 % of the adsorbed CH_4 remains when the pressure further reduced to 25 mmHg. Such a broad desorption behaviour for CH_4 isotherm at atmospheric pressure is rarely observed in microporous MOFs.[11,17] After CH_4 uptake the PXRD pattern of **IFP-8** maintained its structural integrity. The structural transformation was not occurred (Fig. S10, ESI†). Another agreeable example that has proven the flexibility of the framework is by H_2 sorption. **IFP-8** adsorbs 9.3 cm^3 g^{-1} of H_2 at 77 K and 1 bar (Fig. 2a), showing a wide desorption hysteresis. Moreover, we determined the initial slopes in the Henry region of the adsorption isotherms of **IFP-8** (Fig. S13, ESI†). The adsorption selectivities of **IFP-8** are 34:1 and 9:1 for CO_2/N_2 and CO_2/CH_4, respectively, wherein the adsorption selectivities of IFP-7 are 37:1 and 7:1 for CO_2/N_2 and CO_2/CH_4, respectively at 273 K and 1 bar.[11]

In conclusion, not only zinc can formed H-bonded supramolecular assembly but also cobalt yielded a large Co_{14}-MOC via *in situ* functionalization of unusual linker generation under solvothermal condition. The cobalt atoms in the Co_{14}-MOC formed Co_6 octahedron inscribed distorted Co_8 cube (Co_6@Co_8). However, **1** shows the **bcu** net with 14 cobalt atoms. Due to flexible methoxy substituent, the hysteretic sorption behavior for **IFP-8** indicates a flexible MOF. **IFP-8** exhibits the gas sorption selectivity.

We thank Dr. I. A. Baburin (Institut für Physikalische Chemie und Elektrochemie, Technische Universität Dresden, Dresden, Germany) for theoretical calculations for **IFP-8**. This work is financially supported by the Priority Program 1362 of the German Research Foundation on "Metal-Organic Frameworks."

Notes and references

1 J. W. Steed and J. L. Atwood in *Supramolecular Chemistry*, 2nd Edition, Wiley-VCH, Weinheim, Germany, 2009.
2 (*a*) L. R. MacGillivray in *Metal-Organic Frameworks: Design and Application*, John Wiley & Sons, Hoboken, NJ, 2010; (*b*) D. Farrusseng, in *Metal-Organic Frameworks Applications from Catalysis to Gas Storage*, Wiley-VCH, Weinheim, Germany, 2011.
3 C.-L. Chen and A. M. Beatty, *J. Am. Chem. Soc.,* 2008, **130**, 17222–17223.
4 G. A. Hogan, N. P. Rath and A. M. Beatty, *Cryst. Growth Des.,* 2011, **11**, 3740–3743.
5 D. F. Sava, V. Ch. Kravtsov, J. Eckert, J. F. Eubank, F. Nouar and M. Eddaoudi, *J. Am. Chem. Soc.,* 2009, **131**, 10394–10396.
6 S. Wang, T. Zhao, G. Li, L. Wojtas, Q. Huo, M. Eddaoudi and Y. Liu, *J. Am. Chem. Soc.,* 2010, **132**, 18038–18041.
7 (*a*) S. Kitagawa and K. Uemura, *Chem. Soc. Rev*., 2005, **34**, 109−119; (*b*) G. Férey and C. Serre, *Chem. Soc. Rev*., 2009, **38**, 1380−1399.
8 (*a*) J.-R. Li, J. Sculley and H.-C. Zhou, *Chem. Rev*., 2012, **112**, 869−932; (*b*) L. E. Kreno, K. Leong, O. K. Farha, M. Allendorf, R. P. Van Duyne and J. T. Hupp, *Chem. Rev*., 2012, **112**, 1105−1125.
9 (*a*) S. Henke, A. Schneemann, A. Wu□tscher and R. A. Fischer, *J. Am. Chem. Soc*., 2012, **134**, 9464−9474; (*b*) S. Henke and R. A. Fischer, *J. Am. Chem. Soc*., 2011, **133**, 2064–2067.
10 (*a*) F. Debatin, A. Thomas, A. Kelling, N. Hedin, Z. Bacsik, I. Senkovska, S. Kaskel, M. Junginger, H. Müller, U. Schilde, C. Jäger, A. Friedrich and H.-J. Holdt, *Angew. Chem. Int. Ed.*, 2010, **49**, 1258–1262; (*b*) F. Debatin, K. Behrens, J. Weber, I. A. Baburin, A. Thomas, J. Schmidt, I. Senkovska, S. Kaskel, A. Kelling, N. Hedin, Z. Bacsik, S. Leoni, G. Seifert, C. Jäger, C. Günter, U. Schilde, A. Friedrich and H.-J. Holdt, *Chem. Eur. J.*, 2012, **18**, 11630–11640.
11 S. S. Mondal, A. Bhunia, I. A. Baburin, C. Jäger, A. Kelling, U. Schilde, G. Seifert, C. Janiak and H.-J. Holdt, *Chem. Commun.*, 2013, **49**, 7599–7601.
12 S. S. Mondal, A. Bhunia, S. Demeshko, A. Kelling, U. Schilde, C. Janiak and H.-J. Holdt, *CrystEngComm*., 2104, **16**, 39–42.
13 S. S. Mondal, A. Bhunia, A. Kelling, U. Schilde, C. Janiak and H.-J. Holdt, *J. Am. Chem. Soc.*, 2014, **136**, 44–47.
14 T. D. Keene, D. J. Price and C. J. Kepert, *Dalton Trans*., 2011, **40**, 7122–7126.
15 Crystal data for **1**: $C_{14.50}H_{22.25}Co_{1.75}N_{8.50}O_{7.37}$, Mr = 536.78 g·mol^{-1}, crystal dimensions 0.44 × 0.42 × 0.40 mm, tetragonal, space group $I4/m$(No 87), $a = b$ = 17.8029(3) Å, c = 29.2271(7) Å, V = 9263.3(4) $Å^3$, Z = 16, ρ_{calcd} = 1.54 g·cm^{-3}; $\mu(Mo_{K\alpha})$ = 1.313 mm^{-1} (λ = 0.71073 Å), T = 210 K; $2\Theta_{max}$ = 25.00°, 29163 reflections measured, 4156 unique (R_{int} = 0.1056), R_1 = 0.0623, wR = 0.1750 ($I > 2\sigma(I)$).
16 T. Panda, K. M. Gupta, J. Jiang and R. Banerjee, *CrystEngComm*., 2014, DOI: 10.1039/C3CE42075B.
17 D. Zhao, D. Yuan, R. Krishna, J. M. van Baten and H.-C. Zhou, *Chem. Commun.,* 2010, **46**, 7352–7354.

[a] *Institut für Chemie, Anorganische Chemie, Universität Potsdam, Karl-Liebknecht-Straße 24-25, 14476 Potsdam, Germany*
Fax: +49 331-977-5055; Tel: +39 331-977-5180; E-mail: holdt@uni-potsdam.de
[b] *Institut für Anorganische Chemie und Strukturchemie, Heinrich-Heine-Universität Düsseldorf, 40204 Düsseldorf, Germany*

† Electronic Supplementary Information (ESI) available: Detailed experimental procedure, IR spectra, PXRD patterns, TGA traces, table of X-ray data of **1**, gas adsorption data. CCDC 974537. See DOI: 10.1039/b000000x/‡